

Gohberg-Semencul Estimation of Toeplitz Structured Covariance Matrices and Their Inverses

Benedikt Böck, *Graduate Student Member, IEEE*, Dominik Semmler, *Graduate Student Member, IEEE*,
Benedikt Fesl, *Graduate Student Member, IEEE*, Michael Baur, *Graduate Student Member, IEEE*,
and Wolfgang Utschick, *Fellow, IEEE*

Abstract—When only few data samples are accessible, utilizing structural prior knowledge is essential for estimating covariance matrices and their inverses. One prominent example is knowing the covariance matrix to be Toeplitz structured, which occurs when dealing with wide sense stationary (WSS) processes. This work introduces a novel class of positive definiteness ensuring likelihood-based estimators for Toeplitz structured covariance matrices (CMs) and their inverses. In order to accomplish this, we derive positive definiteness enforcing constraint sets for the Gohberg-Semencul (GS) parameterization of inverse symmetric Toeplitz matrices. Motivated by the relationship between the GS parameterization and autoregressive (AR) processes, we propose hyperparameter tuning techniques, which enable our estimators to combine advantages from state-of-the-art likelihood and non-parametric estimators. Moreover, we present a computationally cheap closed-form estimator, which is derived by maximizing an approximate likelihood. Due to the ensured positive definiteness, our estimators perform well for both the estimation of the CM and the inverse covariance matrix (ICM). Extensive simulation results validate the proposed estimators' efficacy for several standard Toeplitz structured CMs commonly employed in a wide range of applications.

Index Terms—Covariance estimation, autoregressive processes, Gohberg-Semencul, Toeplitz, likelihood estimation.

I. INTRODUCTION

Second moments in the form of the CM and its inverse characterize the statistical properties of random variables and, thus, play a fundamental role in statistical signal processing. They are used in a wide range of applications to extract the desired information from collected data, including linear estimation, prediction, dimensionality reduction, and clustering [1, Ch. 1-2], [2, Ch. 3-4], [3]. In practical settings, however, the required second moments are usually unknown and must be estimated [1, Ch. 3], [3]. A basic unbiased estimator of the CM is the sample covariance matrix (SCM), which yields good performance in cases where many data samples are accessible. Nevertheless, its slowly decaying mean squared error (MSE) makes it unreliable in scenarios where the number of available data samples is small [4, Sec. 2.2]. Furthermore, in cases where the number of data samples is even smaller than their dimension, the SCM becomes singular and, thus, cannot be directly used for estimating the ICM. Prominent examples of applications in which generally only a very limited amount

of samples is available are, e.g., financial engineering [5], array signal processing [6], biological inference, and social networks [7], [8]. Thus, many different estimators for the CM and ICM based on few samples have been developed over the last decades.

In this paper, we consider the problem of estimating Toeplitz structured CMs and their inverses, constituting a large subclass of second moments. Toeplitz structures arise when a WSS random process is sampled equidistantly. This occurs in, e.g., sensor arrays capturing samples of a WSS spatial process or sampling a WSS time-varying signal. Many problems in imaging [9], array signal processing [10], speech and audio processing [11], geostatistics [12], and medical applications [13] fit into this category. Moreover, many non-stationary processes in, e.g., wireless communication [14, Sec. 2.3], speech processing [15], and finance [16], can be assumed to be quasi-stationary and, thus, also exhibit a locally concentrated Toeplitz structure within their second moments.

Exploiting structural knowledge for estimating CMs was first considered in [17] and [18], in which conditions for gradient-based updates of the structured CM are derived to maximize the Gaussian likelihood. The main focus in these publications lies on CMs that can be linearly decomposed by a dictionary of pre-known basis matrices (e.g., Toeplitz). Another likelihood estimator, proposed in [19], considers the available samples as incomplete observations from data samples with larger dimension and a corresponding circulant CM. Enforcing the CM to be circulant exhibits a closed-form solution for the likelihood's maximizer and allows a computationally efficient way to estimate the Toeplitz structured CM by applying the expectation-maximization (EM) algorithm for incomplete data [20].

A different approach to estimate Toeplitz structured CMs is to exploit their property to be constant along the diagonals and to take the SCM averaged along its diagonals (SAVG) as CM estimate [21]. Compared to likelihood estimators, this idea has the advantage that it neither assumes any underlying distribution nor requires solving an optimization problem (OP). On the other hand, averaging along the diagonals does not necessarily preserve the CM's property of positive semidefiniteness. Additionally, as the distance from the off-diagonal to the main-diagonal increases, fewer samples are considered for averaging, resulting in a higher variance error. For that reason, the regularization techniques of banding and tapering the estimator have been analyzed [21]. Banding describes the method of setting all matrix entries to zero in

The authors are with Lehrstuhl für Methoden der Signalverarbeitung, Technische Universität München, 80333 München, Germany (e-mail: benedikt.boeck@tum.de; dominik.semmler@tum.de; benedikt.fesl@tum.de; mi.baur@tum.de; utschick@tum.de).

all off-diagonals above a certain bound. Tapering generalizes banding and multiplies the entries along the off-diagonals with decaying weights rather than setting a hard threshold. These techniques were first proposed for the SCM, introducing a bias and leveraging the bias-variance trade-off [22], [23]. A further advantage of these non-parametric estimators is that they perform well in the limit of just one sample [24], [25], which is typically the setup in time series analysis [26]. Another way of regularization is to shrink the SCM towards the SAVG, i.e., to build an optimized convex combination of both [27]. This idea was first proposed in [28] for cases without prior structural information and improved in [29] for Gaussian distributions. Generally, the adjustment of the convex weighting is based on a minimization of the estimated MSE.

A closely related topic to estimating Toeplitz structured CMs is parameter estimation of WSS AR processes in case of observing one sample [30, Ch. 6]. By applying the GS decomposition, estimating the parameters of an AR process implicitly yields an estimate of the ICM (cf. Section V). However, due to the difficulty to optimize the exact likelihood of AR processes, the standard approach is to optimize the sample's conditional (approximate) likelihood by assuming initially observed entries to be deterministic, leading to a least squares (LS) problem [31, Ch. 5]. The resulting ICM estimator, however, cannot be guaranteed to be positive definite (PD) and, thus, inverting can yield arbitrarily bad CM estimates.

This work introduces a novel class of positive definiteness ensuring likelihood estimators for Toeplitz structured CMs and their inverses by utilizing the GS parameterization for inverse symmetric Toeplitz matrices [32] and, thus, by effectively fitting an AR process to the observed data. The closest work to ours is [33], which also yields an exact likelihood estimator based on the GS decomposition. However, this method cannot efficiently distinguish solutions yielding positive definite and indefinite CMs and is either intractable for higher order AR processes or only converges if the initialization is "sufficiently" close to the exact solution. In summary, our main contributions are the following:

- We derive multiple positive definiteness ensuring constraint sets for the GS parameterization. These sets include simple box constraints, offering an efficient means of formulating computationally cheap likelihood-based estimators and integrating additional prior knowledge.
- We introduce hyperparameter tuning techniques enabling our estimators to share benefits from both state-of-the-art likelihood and non-parametric estimators.
- We establish an exact likelihood estimator, which provably converges to a local optimum and whose complexity only scales quadratically with the samples' dimension.
- We propose a computationally cheap closed-form estimator based on an approximate likelihood.

Notation: We begin indexing matrices and vectors with zero unless explicitly specified otherwise. We utilize a special case of the generalized Fibonacci sequence from [34] denoted as

$$\begin{aligned} F_0(\mathbf{r}) &= 1 \\ F_i(\mathbf{r}) &= \sum_{l=0}^{i-1} r_{i-l} F_l(\mathbf{r}) \text{ for all } i \in \{1, \dots, P\}. \end{aligned} \quad (1)$$

In this particular scenario, the vector $\mathbf{r} = [r_1, \dots, r_P]^T$ begins with the index 1. The set of strictly positive real valued numbers, the set of strictly positive natural numbers and the convex cone of Hermitian $P \times P$ PD matrices are denoted by \mathbb{R}_{++} , \mathbb{N} and \mathbb{S}_{++}^P , respectively. The complex conjugate of $\beta \in \mathbb{C}$ is given by $\bar{\beta}$ and the operator \mathbf{E} denotes the shift-down matrix, defined by its entries $E_{ij} = \delta(i-1-j)$ with $\delta(\cdot)$ being the Kronecker delta. We write the indicator function as $\chi(\cdot)$, which is one if the argument is true and zero otherwise. Moreover, by $|\mathbf{r}|$ we indicate the vector, which contains the entries of \mathbf{r} in absolute value and the i, j th entry in some matrix \mathbf{A} is denoted by A_{ij} . Additionally, by writing $\mathbf{A}_{\geq i, \geq j}$ or $\mathbf{r}_{\geq k}$, we refer to the submatrix or subvector of \mathbf{A} or \mathbf{r} , starting at row index i and column index j , or index k , respectively.

II. PROBLEM FORMULATION

Let $\mathcal{D} = \{\mathbf{x}^{(n)}\}_{n=1}^N$ be a set of N independent and identically distributed (i.i.d.) real or complex-valued samples drawn from a P -dimensional mean-zero Gaussian distribution with a full-rank Toeplitz structured CM \mathbf{C} . This work aims to find an estimator $\hat{\Gamma}(\mathcal{D})$ for the ICM $\Gamma = \mathbf{C}^{-1}$, given the dataset \mathcal{D} and assuming N either smaller or in the range of P . Likelihood estimators maximize the probability density of the collected data over a parameter space containing all allowed configurations of the estimator. For our given setup, the likelihood estimator equals

$$\hat{\Gamma}(\mathcal{D}) = \underset{\Gamma}{\operatorname{argmax}} \prod_{n=1}^N \mathcal{N}(\mathbf{x}_n; \mathbf{0}, \Gamma^{-1}) \text{ s.t. } \Gamma \in \mathcal{G} \quad (2)$$

with \mathcal{G} containing all inverses of PD Hermitian Toeplitz matrices. After a few reformulations, by neglecting constants and introducing the SCM $\mathbf{S} = 1/N \sum_{n=1}^N \mathbf{x}_n \mathbf{x}_n^H$, the OP in (2) can be stated as

$$\hat{\Gamma}(\mathcal{D}) = \underset{\Gamma}{\operatorname{argmax}} \log \det \Gamma - \operatorname{tr}(\Gamma \mathbf{S}) \text{ s.t. } \Gamma \in \mathcal{G}. \quad (3)$$

We specify the constraint set \mathcal{G} by using the GS decomposition for symmetric Toeplitz matrices [32]. After a minor extension to the complex-valued case, it states that a matrix \mathbf{T}^{-1} is the inverse of a full-rank but not necessarily PD Hermitian Toeplitz matrix $\mathbf{T} \in \mathbb{C}^{P \times P}$ if and only if it exhibits a decomposition in the following form

$$\mathbf{T}^{-1} = \frac{1}{\alpha_0} (\mathbf{B}\mathbf{B}^H - \mathbf{Z}\mathbf{Z}^H), \quad (4)$$

where \mathbf{B} and \mathbf{Z} are defined as

$$\mathbf{B} = \begin{pmatrix} \alpha_0 & 0 & 0 & \dots & 0 \\ \alpha_1 & \alpha_0 & 0 & \dots & 0 \\ \dots & \dots & \dots & \dots & \dots \\ \alpha_{P-1} & \alpha_{P-2} & \alpha_{P-3} & \dots & \alpha_0 \end{pmatrix} \quad (5)$$

and

$$\mathbf{Z} = \begin{pmatrix} 0 & 0 & 0 & \dots & 0 \\ \frac{1}{\alpha_{P-1}} & 0 & 0 & \dots & 0 \\ \dots & \dots & \dots & \dots & \dots \\ \frac{1}{\alpha_1} & \frac{1}{\alpha_2} & \dots & \frac{1}{\alpha_{P-1}} & 0 \end{pmatrix}. \quad (6)$$

The parameter α_0 has to be real-valued and positive while the residual parameters $\alpha_1, \dots, \alpha_{P-1}$ are unconstrained. We

reparameterize the OP in (3) by enforcing $\mathbf{\Gamma}$ to satisfy the GS formula in (4). By defining the corresponding log-likelihood $\mathcal{L}_{\mathcal{D}}(\boldsymbol{\alpha})$ as

$$\mathcal{L}_{\mathcal{D}}(\boldsymbol{\alpha}) = \log \det \mathbf{\Gamma}(\boldsymbol{\alpha}) - \text{tr}(\mathbf{\Gamma}(\boldsymbol{\alpha})\mathbf{S}), \quad (7)$$

and including the positive definiteness of $\mathbf{\Gamma}(\boldsymbol{\alpha})$ as constraint, the likelihood estimation reads as

$$\begin{aligned} \hat{\boldsymbol{\alpha}}(\mathcal{D}) &= \underset{\boldsymbol{\alpha}}{\text{argmax}} \mathcal{L}_{\mathcal{D}}(\boldsymbol{\alpha}) \\ \text{s.t. } \boldsymbol{\alpha} &\in \mathcal{G}_{\alpha} = \{\boldsymbol{\alpha} \in \mathbb{R}_{++} \times \mathbb{C}^{P-1} : \mathbf{\Gamma}(\boldsymbol{\alpha}) \in \mathbb{S}_{++}^P\} \end{aligned} \quad (8)$$

with $\hat{\mathbf{\Gamma}}(\mathcal{D}) = \mathbf{\Gamma}(\hat{\boldsymbol{\alpha}}(\mathcal{D}))$. Due to the impractical formulation of \mathcal{G}_{α} for applying standard optimization algorithms, the OP for the exact log-likelihood in (8) is generally ill-posed [33] [31, Sec. 5.9]. Thus, we reformulate \mathcal{G}_{α} in the following to end up with a well-defined OP.

III. RELATED WORK

In this section, we give a summary about other methods used for estimating Toeplitz structured CMs. Generally, these estimators can be classified into likelihood estimators, banding and tapering estimators, and shrinkage estimators.

A. Likelihood Estimators

In existing literature, the proposed likelihood estimators for Toeplitz structured CMs aim to identify the optimizer

$$\hat{\mathbf{C}} = \underset{\mathbf{C} \in \mathcal{C}_{\text{T}}}{\text{argmax}} -\log \det \mathbf{C} - \text{tr}(\mathbf{C}^{-1}\mathbf{S}) \quad (9)$$

with \mathcal{C}_{T} containing all positive semidefinite Hermitian Toeplitz structured matrices and, thus, they estimate directly the CM. The work in [19] builds on the insights from [18] and interprets the observed P -dimensional samples as incomplete observations from a G -periodic process with a $G \times G$ circulant CM, with $G > P$. As circulant matrices can be diagonalized by the discrete Fourier transform (DFT) matrix \mathbf{F}_G , the Gaussian likelihood enables a closed-form optimization for circulant CMs, given by

$$\hat{\mathbf{C}}_{\text{Circ}} = \mathbf{F}_G^{\text{H}} \text{diag}(\mathbf{F}_G \mathbf{S}_C \mathbf{F}_G^{\text{H}}) \mathbf{F}_G. \quad (10)$$

However, the $G \times G$ SCM \mathbf{S}_C is intractable due to only incomplete subsamples of dimension P being observed. To address this problem, an iterative EM algorithm is derived based on the work in [20], which consists of repeating the following step:

$$\hat{\boldsymbol{\Sigma}}^{(t+1)} = \text{diag}(\hat{\boldsymbol{\Sigma}}^{(t)} \tilde{\mathbf{F}}_G \hat{\mathbf{C}}_p^{(t)-1} \mathbf{S} \hat{\mathbf{C}}_p^{(t)-\text{H}} \tilde{\mathbf{F}}_G^{\text{H}} + \hat{\boldsymbol{\Sigma}}^{(t)} - \hat{\boldsymbol{\Sigma}}^{(t)} \tilde{\mathbf{F}}_G \hat{\mathbf{C}}_p^{(t)-1} \tilde{\mathbf{F}}_G^{\text{H}} \hat{\boldsymbol{\Sigma}}^{(t)\text{H}}), \quad (11)$$

where $\hat{\boldsymbol{\Sigma}}^{(t)}$ is the estimated $G \times G$ Fourier transformed circulant CM in the t th iteration, $\tilde{\mathbf{F}}_G$ is the left $G \times P$ submatrix of \mathbf{F}_G , \mathbf{S} is the $P \times P$ SCM of the observations, and $\hat{\mathbf{C}}_p^{(t)}$ is the left upper $P \times P$ submatrix of $\mathbf{F}_G \hat{\boldsymbol{\Sigma}}^{(t)} \mathbf{F}_G^{\text{H}}$ and, thus, an estimator of the $P \times P$ Toeplitz structured CM in the t th iteration. After reaching a termination criterion in the T th iteration, $\hat{\mathbf{C}}_p^{(T)}$ is considered as the estimate of the CM and will be denoted by $\hat{\mathbf{C}}_{\text{EM}}$.

Finally, by assuming $G = P$ and substituting the SCM \mathbf{S} for \mathbf{S}_C , the closed-form likelihood estimator $\hat{\mathbf{C}}_{\text{Circ}}$ in (10) is considered as another likelihood estimate.

B. Banding and Tapering Estimators

Initially, the method of banding and tapering was applied to the SCM to reduce its MSE [22]. In both cases, the operation consists of an elementwise multiplication of the SCM \mathbf{S} with a specific mask matrix \mathbf{M} , i.e.,

$$\hat{\mathbf{C}} = \mathbf{M} \odot \mathbf{S}. \quad (12)$$

In case of banding, the mask matrix \mathbf{M} is given by

$$\mathbf{M}_{ij} = \chi(|i - j| \leq k_{\text{B}}), \quad (13)$$

with k_{B} being a hyperparameter and $\chi(\cdot)$ being the indicator function. Tapering, on the other hand, is a generalization of banding, in which we allow a windowing function $g(\cdot)$ of choice determining the entries \mathbf{M}_{ij} , i.e.,

$$\mathbf{M}_{ij} = g(|i - j|). \quad (14)$$

The work in [21] investigates banding and tapering for estimating Toeplitz structured CMs by exchanging the SCM with the SAVG \mathbf{S}_{avg} , i.e.,

$$\mathbf{S}_{\text{avg}} = \frac{\text{tr}(\mathbf{S})}{P} \mathbf{I} + \sum_{q=1}^{P-1} \frac{\text{tr}(\mathbf{S} \mathbf{E}^q)}{P-q} (\mathbf{E}^q)^{\text{T}} + \frac{\overline{\text{tr}(\mathbf{S} \mathbf{E}^q)}}{P-q} \mathbf{E}^q. \quad (15)$$

However, since \mathbf{S}_{avg} is not necessarily positive semidefinite, neither the tapered nor the banded estimator $\hat{\mathbf{C}}$ in (12) are guaranteed to possess this property. Various options exist to address this problem. One possibility is described in [21], which is based on a modification of the corresponding spectral density. However, these methods may yield rank deficient estimators, making them unsuitable for estimating the ICM. In fact, [21] proposes an ICM estimator, which is optimal with respect to its convergence rate. However, this estimator suffers from requiring genie knowledge about the true CM. Moreover, it neglects the observations and outputs the identity matrix as ICM estimate if the CM tapering estimator contains an eigenvalue below a certain threshold, which leads to arbitrarily large errors for particular estimates. To our knowledge, no practical method has been proposed in the literature for constructing a well-conditioned banding or tapering based estimator of the ICM. For tuning the hyperparameter, [22] employs k -fold cross validation. However, the case of having one single sample, i.e., $N = 1$, renders k -fold cross validation infeasible and was investigated in [24] and [25]. Instead of using the unbiased estimator \mathbf{S}_{avg} for banding or tapering, the authors consider a biased version \mathbf{S}_{acf} , in which the summation over all entries along a SCM's diagonal is divided by the sample's dimension P , instead of the number of entries. This is usually referred to as sample autocovariance function [26, Sec. 1.4.4]. Additionally, the authors in [24] and [25] introduce tailored methods for hyperparameter tuning.

C. Shrinkage Estimator

The idea of shrinkage estimators is to utilize the bias-variance trade-off and to intentionally incorporate bias by building a convex combination of the unbiased SCM with a biased target matrix \mathbf{T} [28]. The estimator is given by

$$\hat{\mathbf{C}}_{\text{shrink}} = (1 - \rho)\mathbf{S} + \rho\mathbf{T} \quad (16)$$

with shrinkage coefficient $\rho \in [0, 1]$. By minimizing the MSE with respect to ρ , i.e.,

$$\rho_{\text{opt}}(\mathbf{T}, \mathbf{C}) = \underset{\rho \in [0, 1]}{\operatorname{argmin}} \mathbb{E}[\| (1 - \rho)\mathbf{S} + \rho\mathbf{T} - \mathbf{C} \|_F^2], \quad (17)$$

one can find a value, which optimally leverages the bias-variance trade-off. Since $\rho_{\text{opt}}(\mathbf{T}, \mathbf{C})$ depends on the true CM \mathbf{C} , it is intractable and must be estimated. In [29], an estimator $\hat{\rho}$ is proposed for the case of i.i.d. Gaussian data samples and a scaled identity as target matrix, i.e., $\mathbf{T}_1 = \frac{\operatorname{tr}(\mathbf{S})}{P} \mathbf{I}$. The work in [27] introduces \mathbf{S}_{avg} , defined in (15), as a specific target matrix for Toeplitz structured CMs. Since \mathbf{S}_{avg} is also unbiased, taking it as a target does not introduce bias, but still decreases the variance error due to the utilization of structural knowledge. The work in [35] considers another Toeplitz structured target \mathbf{T}_H , which is constant in all off-diagonal entries, and thus, introduces a bias. More precisely,

$$\mathbf{T}_H = \frac{\operatorname{tr}(\mathbf{S})}{P} \mathbf{I} + \frac{\operatorname{tr}(\mathbf{S}\mathbf{H})}{P(P-1)} \mathbf{H} \quad (18)$$

with $\mathbf{H} = \mathbf{1}\mathbf{1}^T - \mathbf{I}$ and $\mathbf{1}$ being the all-ones vector. Due to the positive definiteness of \mathbf{T}_H , the resulting shrinkage estimator is PD. In our simulations, we take the proposed shrinkage coefficient estimators $\hat{\rho}$ in [35] for both targets \mathbf{S}_{avg} and \mathbf{T}_H .

IV. POSITIVE DEFINITENESS CONSTRAINTS FOR THE GS DECOMPOSITION

The goal of this section is to bring (8) into the standard form of OPs, cf. [36, Sec. 1.1]:

$$\max_{\boldsymbol{\alpha}} f(\boldsymbol{\alpha}) \quad \text{s.t.} \quad g_i(\boldsymbol{\alpha}) \leq 0, \quad i = 1, \dots, m \quad (19)$$

with $\boldsymbol{\alpha} \in \mathbb{R} \times \mathbb{C}^{P-1}$. Since α_0 has to be strictly positive, we introduce a small positive constant ϵ_0 serving as a lower bound for α_0 and resulting in the inequality constraint

$$g_1(\boldsymbol{\alpha}) = \epsilon_0 - \alpha_0. \quad (20)$$

It remains to reformulate the condition of $\Gamma(\boldsymbol{\alpha})$ to be PD, which is explained in the following.

A. Eigenvalue Constraints

Various approaches exist to include the constraint of positive definiteness into an OP. The geometric approach of iteratively projecting onto \mathbb{S}_{++}^P , cf. [36, Sec. 8.1.1], is not applicable since our OP is conducted directly over the domain of $\boldsymbol{\alpha}$. Reparameterizing the OP using the Cholesky decomposition of PD matrices [37] also cannot be used due to the restriction to the GS parameterization (4). Alternatively, we can ensure positive definiteness by enforcing positive eigenvalues of $\Gamma(\boldsymbol{\alpha})$ [37], i.e.,

$$\begin{aligned} \hat{\boldsymbol{\alpha}}(\mathcal{D}) &= \underset{\boldsymbol{\alpha}}{\operatorname{argmax}} \mathcal{L}_{\mathcal{D}}(\boldsymbol{\alpha}) \\ \text{s.t.} \quad &\epsilon_0 - \alpha_0 \leq 0 \\ &\epsilon_i - \lambda_i(\Gamma(\boldsymbol{\alpha})) \leq 0, \quad i = 1, \dots, P \end{aligned} \quad (21)$$

with $\lambda_i(\Gamma(\boldsymbol{\alpha}))$ being the i th eigenvalue of $\Gamma(\boldsymbol{\alpha})$. The eigenvalues of a Hermitian matrix are differentiable [38, Th. 6.8], rendering the OP solvable with, e.g., an interior point method.

We introduce small positive constants ϵ_i for each eigenvalue to enforce strict positivity. However, the eigenvalue decomposition in each step takes $\mathcal{O}(P^3)$ floating point operations (FLOPs) and the number of nonlinear inequality constraints scales with P . These observations render the estimator to be computationally infeasible in high-dimensional settings and, thus, more advanced constraint sets are needed.

B. Frobenius-Based Constraint

By inserting the GS decomposition (4) into the definition of positive definiteness and a few reformulations, we obtain the following equivalence.

Lemma 1. *If $\Gamma(\boldsymbol{\alpha})$ satisfies the GS decomposition in (4) and $\mathcal{A} \subseteq \mathbb{R}_{++} \times \mathbb{C}^{P-1}$, then*

$$(\Gamma(\boldsymbol{\alpha}) \in \mathbb{S}_{++}^P \text{ for all } \boldsymbol{\alpha} \in \mathcal{A}) \iff \left(\max_{\boldsymbol{\alpha} \in \mathcal{A}} \|\mathbf{Z}^H \mathbf{B}^{-H}\|_2^2 < 1 \right) \quad (22)$$

with \mathbf{B} and \mathbf{Z} given by (5) and (6), respectively.

Proof. See Appendix A. \square

Lemma 1 can be utilized to reformulate the OP (21) to just having two inequality constraints independently of the samples' dimension P . The spectral norm, however, is not differentiable everywhere [39, Th. 1.1]. One method to overcome this issue is to apply a subgradient method for finding a local optimum. Alternatively, we introduce a differentiable upper bound for the spectral norm, which ensures the differentiability of the constraint. More precisely, we leverage the relationship that the Frobenius norm of a matrix is always greater than or equal to its spectral norm. This allows us to deduce the following implication:

$$\left(\max_{\boldsymbol{\alpha} \in \mathcal{A}} \|\mathbf{Z}^H \mathbf{B}^{-H}\|_F^2 < 1 \right) \Rightarrow (\Gamma(\boldsymbol{\alpha}) \in \mathbb{S}_{++}^P \text{ for all } \boldsymbol{\alpha} \in \mathcal{A}). \quad (23)$$

By utilizing (23), we reformulate the OP (8) while preserving the differentiability of the constraint

$$\begin{aligned} \hat{\boldsymbol{\alpha}}(\mathcal{D}) &= \underset{\boldsymbol{\alpha}}{\operatorname{argmax}} \mathcal{L}_{\mathcal{D}}(\boldsymbol{\alpha}) \\ \text{s.t.} \quad &\epsilon_0 - \alpha_0 \leq 0 \\ &\|\mathbf{Z}^H \mathbf{B}^{-H}\|_F^2 - 1 + \epsilon_f \leq 0 \end{aligned} \quad (24)$$

with ϵ_f being a small positive constant enforcing $\|\mathbf{Z}^H \mathbf{B}^{-H}\|_F^2$ to be strictly smaller 1. Both, the inversion of a triangular Toeplitz matrix as well as the multiplication of two upper (lower) triangular Toeplitz matrices preserve the triangular Toeplitz structure [40], [41]. Thus, $\|\mathbf{Z}^H \mathbf{B}^{-H}\|_F^2$ is fully determined by the entries of $\mathbf{B}^{-1} \mathbf{z}_1$, where \mathbf{z}_1 is the first column of \mathbf{Z} . It takes $\mathcal{O}(P^2)$ operations to compute $\mathbf{B}^{-1} \mathbf{z}_1$, leading to a significantly reduced complexity to evaluate the constraint. While the eigenvalue constraints in (21) represent an equivalent reformulation of \mathcal{G}_{α} in (8), the constraint set in OP (24) is a subset of \mathcal{G}_{α} . A smaller constraint set has a stronger regularization effect and generally decreases the estimator's variance. At the same time, it potentially introduces a bias, whose effect can be either beneficial or disadvantageous depending on how well the smaller constraint set can cover

the estimator's most relevant features. In our simulations, we either observed similar or even better performance by taking the constraint set in (24) instead of (21), rendering it well suited for the problem at hand.

C. Box Constraints

Convexity is generally a desirable property for the constraint set because it allows for projecting onto the set by solving a convex OP [36, Sec. 8.1.1]. Box constraints further simplify projections, requiring only $\mathcal{O}(P)$ FLOPs. In the following, we derive box constraints constituting a subset of \mathcal{G}_α and, thus, imposing a stronger regularization. However, they offer an additional means to control this effect by incorporating additional prior knowledge, which will be discussed in more detail in Section V-C and, thus, their advantages extend beyond computational efficiency. We start with the constraint on the Frobenius norm in (24). The matrix \mathbf{B} is a lower triangular Toeplitz matrix for which the inverse can be computed by means of the generalized Fibonacci polynomials [34]. By utilizing this connection, we derive the following relation.

Lemma 2. *Let \mathbf{B} and \mathbf{Z} be defined according to (5) and (6), respectively, then*

$$\|\mathbf{Z}^H \mathbf{B}^{-H}\|_F^2 = \sum_{d=1}^{P-1} (P-d)|g_d|^2 \quad (25)$$

with

$$g_d = \sum_{j=1}^d \frac{\alpha_{P-j}}{\alpha_0} F_{d-j} \left(-\frac{\alpha_{\geq 1}}{\alpha_0} \right) \quad \text{for all } d = 1, \dots, P-1, \quad (26)$$

and $F_i(\cdot)$ being the special case of the generalized Fibonacci sequence in (1).

Proof. See Appendix B. \square

Motivated by the observation that (26) only depends on α through fractions of the form α_i/α_0 ($i > 0$), we introduce the following box constraints

$$\left| \frac{\alpha_i}{\alpha_0} \right| \leq K_i, \quad K_i > 0 \quad \text{for all } i = 1, \dots, P-1. \quad (27)$$

By means of Lemma 2 and the bounds in (27), we derive the following Theorem, which guarantees the existence of positive definiteness enforcing box constraints.

Theorem 1. *Let $\Gamma(\alpha)$ satisfy the GS decomposition in (4) and let $\tilde{\mathcal{A}}$ be defined as*

$$\tilde{\mathcal{A}} = \{ \alpha \in \mathbb{R}_{++} \times \mathbb{C}^{P-1} : |\alpha_i| \leq K_i \alpha_0 \text{ for all } i = 1, \dots, P-1 \}. \quad (28)$$

Moreover, let $\mathbf{K} = [K_1, \dots, K_{P-1}]^T$ and $B(\mathbf{K})$ satisfy

$$B(\mathbf{K}) = \sum_{d=1}^{P-1} (P-d) \left(\sum_{j=1}^d K_{P-j} F_{d-j}(\mathbf{K}) \right)^2. \quad (29)$$

Then,

$$\exists \mathbf{K} \in \mathbb{R}_{++}^{P-1} : B(\mathbf{K}) < 1 \quad (30)$$

with $B(\mathbf{K})$ exhibiting the following property:

$$(B(\mathbf{K}) < 1) \Rightarrow (\Gamma(\alpha) \in \mathbb{S}_{++}^P \text{ for all } \alpha \in \tilde{\mathcal{A}}). \quad (31)$$

Proof. See Appendix C. \square

The property of $B(\mathbf{K})$ in (31) provides a means to determine specific values for \mathbf{K} . To do so, we propose introducing a functional dependency between the entries of \mathbf{K} , which not only simplifies the computation but also provides the possibility to incorporate additional prior knowledge, as discussed in more detail in Section V-C. However, to ensure the existence of the resulting box constraints, we limit ourselves to a specific class of functions. The formal statement of this restriction is provided in the following Lemma.

Lemma 3. *Let f be a function with the following properties*

- a) $f(\eta, i) : \mathbb{R}_+ \times \mathbb{N} \rightarrow \mathbb{R}_+$,
- b) $f(0, i) = 0$ for all $i \in \mathbb{N}$,
- c) $f(\eta, i)$ is continuous and monotonically increasing in η .

Additionally, let $\mathbf{f}(\eta) = [f(\eta, 1), f(\eta, 2), \dots, f(\eta, P-1)]^T$, $\Gamma(\alpha)$ satisfy the GS decomposition in (4), $\tilde{\mathcal{A}}$ be defined according to (28) with

$$K_i = f(\eta, i) \quad \text{for all } i = 1, \dots, P-1, \quad (32)$$

and $B_f(\eta)$ be defined as the concatenation of $B(\cdot)$ in (29) and $\mathbf{f}(\eta)$, i.e., $B_f(\eta) = B(\mathbf{f}(\eta))$. Then

$$\exists \eta \in \mathbb{R}_{++} : B_f(\eta) < 1 \quad (33)$$

with $B_f(\eta)$ exhibiting the following property

$$(B_f(\eta) < 1) \Rightarrow (\Gamma(\alpha) \in \mathbb{S}_{++}^P \text{ for all } \alpha \in \tilde{\mathcal{A}}). \quad (34)$$

Proof. See Appendix D. \square

Lemma 3 simplifies the task of determining the vector-valued \mathbf{K} to deciding for a single value η to fully determine the constraint set. We propose to select the largest possible η for which $B_f(\eta) < 1$, since this leads to the largest possible constraint set within all possible sets satisfying (28) and (32). The function $B_f(\eta)$ is constructed to be monotonically increasing in η and, thus, the parameter η can be precomputed by bisection, i.e., we search for a η for which

$$1 - \epsilon_\eta \leq B_f(\eta) < 1 \quad (35)$$

holds with ϵ_η being a small positive tolerance parameter. In the case of no prior knowledge, the function f could be chosen to constrain all parameters equally, i.e.,

$$f(\eta, i) = \eta. \quad (36)$$

In case of prior knowledge, however, it is possible to choose more sophisticated functions f , which will be discussed in Section V-C. For solely real-valued α_i ($i > 0$), we obtain the following OP by integrating the box constraints (27) into (8):

$$\begin{aligned} \hat{\alpha}(\mathcal{D}) &= \operatorname{argmax}_{\alpha} \mathcal{L}_{\mathcal{D}}(\alpha) \\ \text{s.t. } & \epsilon_0 - \alpha_0 \leq 0 \\ & \alpha_i - K_i \alpha_0 \leq 0 \quad \text{for all } i = 1, \dots, P-1 \\ & -\alpha_i - K_i \alpha_0 \leq 0 \quad \text{for all } i = 1, \dots, P-1, \end{aligned} \quad (37)$$

which can be solved by, e.g., a projected gradient descent. To ensure the box constraints (27) in the complex-valued case, one possibility is to bound the imaginary and real part of α_i/α_0 in absolute value equally by $K_i/2$.

V. RELATION TO AUTOREGRESSIVE PROCESSES AND HYPERPARAMETER TUNING

A. Relation to Autoregressive Processes

Let

$$X_t = \sum_{i=1}^w a_i X_{t-i} + e_t \quad (38)$$

be an AR(w) process of order w with additive white Gaussian noise (AWGN) $e_t \sim \mathcal{N}_{\mathbb{C}}(0, \sigma^2)$. The second moments of AR processes can be put into relation with its parameters by the Yule-Walker equations

$$c(j) = \sum_{i=1}^w a_i c(i-j) + \delta(j)\sigma^2 \text{ for all } j = 0, \dots, w \quad (39)$$

with $c(j)$ being the autocovariance sequence [42, Sec. 2.1.3]. By rewriting (39) as a system of linear equations in matrix vector form with $\mathbf{C}_{ij} = c(i-j)$ being the CM of a $w+1$ -dimensional sample of the process and by inserting the GS parameterization (4) for \mathbf{C}^{-1} , we observe the following relation

$$\alpha_0 = \frac{1}{\sigma^2}, \quad \alpha_i = -\frac{a_i}{\sigma^2} \text{ for all } i = 1, \dots, w. \quad (40)$$

The relationship between the GS parameterization and the parameters of an AR process was initially explored in [43], establishing an interpretability of the former in terms of the latter. Building upon this interpretability, we leverage it to propose techniques for tuning the hyperparameters of our proposed estimators.

B. Order Tuning

Irrespective of the chosen constraint set from Section IV, we propose using the Bayesian information criterion (BIC) for tuning the number of nonzero α_i ($i > 0$). The BIC is commonly utilized to select the statistical model for likelihood estimation out of a set of potential models, whether there is only $N = 1$ or $N > 1$ observations [26, Sec. 5.5.2], [44, Sec. 4.4.1]. For our setup and $N > 1$, the BIC reads as

$$i_{\text{BIC}} = \underset{i \in \{1, \dots, P\}}{\operatorname{argmin}} i \log N - \mathcal{L}_i(\hat{\boldsymbol{\alpha}}_i(\mathcal{D})) \quad (41)$$

with $\mathcal{L}_i(\hat{\boldsymbol{\alpha}}_i(\mathcal{D}))$ being the log-likelihood evaluated at the estimator $\hat{\boldsymbol{\alpha}}_i(\mathcal{D}) \in \mathbb{R}^i$ obtained by optimizing the OP of choice in Section IV. To evaluate the i th log-likelihood, we set the last $P-i$ parameters $\{\alpha_h\}_{h=i}^{P-1}$ in the GS decomposition (4) to zero and optimize solely over the remaining i parameters $\{\alpha_h\}_{h=0}^{i-1}$. Based on the connection between the GS parameterization and AR processes, cf. Section V-A, setting only the first i parameters to nonzero is equivalent to fitting an AR process of order $i-1$ to the available dataset. Moreover, using the BIC for order tuning results in a duality between our estimators and banding estimators, which is explained in Section VII.

C. Box Constraint Tuning

When employing the box constraints discussed in Section IV-C, the function $f(\eta, i)$, detailed in Lemma 3, is an additional hyperparameter and must be determined. The GS parameters are proportional to those of an AR process (cf. Section V-A), so constraining the former implies constraining the latter. Consequently, by fixing a functional dependency between the bounds for the parameters of the GS decomposition, we implicitly assume the same functional dependency between the bounds for the parameters of the AR process. Therefore, by setting $f(\eta, i)$, we effectively exclude certain parameter constellations of the AR process, which we fit to the given dataset.

The way this insight can be incorporated in determining $f(\eta, i)$ depends on the degree of prior knowledge. If, e.g., the concrete functional dependency of the underlying AR process is pre-known, we can decide for one single $f(\cdot, \cdot)$. However, in cases where only limited prior knowledge is given or it is unknown if the true process exhibits a perfect AR structure, relying on one $f(\cdot, \cdot)$ might be too restrictive. In such cases, we propose to decide for a class of functions $\{f_m(\eta_m, i)\}_{m=1}^M$ and to select the one leading to the estimator which maximizes a certain quality measure. One example is the class of exponentially decreasing functions, expressed as

$$f_m(\eta_m, i) = \eta_m \cdot e^{-\lambda_m i} \quad (42)$$

with coefficient $\lambda_m > 0$. This class of functions is motivated by a general understanding of typical AR processes, where the parameters tend to decrease with growing i . One can take the likelihood value of the resulting estimators as quality measure. Alternatively, one can also apply k -fold cross validation [44, Sec. 1.3].

VI. CONDITIONAL LIKELIHOOD ESTIMATION

In Section II, we introduced the exact unconditioned log-likelihood $\mathcal{L}_{\mathcal{D}}(\boldsymbol{\alpha})$ for estimating the GS, cf. (7), and implicitly the AR parameters of any fixed order w . On the other hand, it has been shown that maximizing the conditional likelihood of one observed sample, i.e., $N = 1$, conditioned on its first w (i.e., the order of the fitted AR process) entries comes with the benefit of providing a closed form solution of the estimated AR parameters [31, Sec. 5.3]. However, this estimate cannot guarantee the corresponding ICM estimate to be PD and, thus, no well-conditioned Toeplitz structured CM estimator can be directly inferred. In a first step towards combining this insight with our results from Section IV and V to yield a computationally cheap closed form PD estimator of the ICM as well as the CM, we adapt the setting to the complex-valued and more general case of having $N \geq 1$ samples. More precisely, let $\mathcal{D}_C = \{\mathbf{x}_{<w}^{(n)}\}_{n=1}^N$ and $\mathcal{D}_L = \{\mathbf{x}_{\geq w}^{(n)}\}_{n=1}^N$, then the conditional log-likelihood $\mathcal{L}_{L|C}(\mathbf{a}, \sigma^2)$ of \mathcal{D}_L conditioned on \mathcal{D}_C with respect to the AR parameters $\mathbf{a} = [a_1, \dots, a_w]^T$ and σ^2 , cf. Section V-A, reads as [31, Sec. 5.3]

$$\mathcal{L}_{L|C} = -(P-w) \log(\sigma^2) - \frac{\sum_{n=1}^N \|\mathbf{x}_{\geq w}^{(n)} - \boldsymbol{\mu}_c^{(n)}(\mathbf{a})\|_2^2}{\sigma^2 N} \quad (43)$$

with the i th entry of $\boldsymbol{\mu}_c^{(n)}$ being $\sum_{m=1}^w a_m x_{i-m}^{(n)}$ and $x_{i-m}^{(n)}$ representing the $(i-m)$ th entry of $\mathbf{x}^{(n)}$. By extending the derivation of the closed form estimator for the AR parameters from [30, Sec. 6.5.1], we establish the following relation.

Lemma 4. *Let $\mathcal{L}_{L|C}(\mathbf{a}, \sigma^2)$ be defined according to (43). Then, the maximizers $\hat{\mathbf{a}}$ and $\hat{\sigma}^2$ of $\mathcal{L}_{L|C}(\mathbf{a}, \sigma^2)$ satisfy*

$$\hat{\mathbf{a}} = \tilde{\mathbf{S}}_{\geq 1, \geq 1}^{-1} \tilde{\mathbf{S}}_{\geq 1, 0}, \quad \hat{\sigma}^2 = \frac{1}{P-w} \left(\tilde{\mathbf{S}}_{0,0} - \tilde{\mathbf{S}}_{\geq 1,0}^H \hat{\mathbf{a}} \right), \quad (44)$$

where $\tilde{\mathbf{S}} \in \mathbb{C}^{w+1 \times w+1}$ is defined as

$$\tilde{S}_{j,l} = \sum_{t=w}^{P-1} \mathbf{S}_{t-l, t-j} \quad (45)$$

with \mathbf{S} being the SCM.

Proof. See Appendix E. \square

The disadvantage of the AR parameter estimates in (44) for estimating the CM is the missing guarantee of positive definiteness of the corresponding ICM. For increasing dimension P , however, the distributions of the exact and conditional likelihood estimator converge to each other [31, Sec. 5.2]. This motivates the assumption that for very large P , the conditional likelihood estimator also provides positive definiteness, which is implicitly assumed in, e.g., [45]. However, there is no mathematical guarantee for finite dimensions, and for small P or close-to-unstable AR processes, this assumption does not hold [30, Sec. 6.5.2]. To overcome this issue, we propose to utilize the derived box constraints in Section IV-C and to project the corresponding GS parameters resulting from (44) and (40) onto this constraint set, i.e.,

$$\hat{\alpha}_{0, \text{PLS}} = \frac{1}{\hat{\sigma}^2}, \quad \hat{\boldsymbol{\alpha}}_{\geq 1, \text{PLS}} = \text{Proj}_{\mathcal{K}} \left(-\frac{1}{\hat{\sigma}^2} \hat{\mathbf{a}} \right), \quad (46)$$

where $\text{Proj}_{\mathcal{K}}(\cdot)$ is the projection onto the box constraints defined by (27), and $\hat{\sigma}^2$ and $\hat{\mathbf{a}}$ are given by (44). The corresponding ICM and CM estimate can then be computed from (4) and are referred to as projected LS (PLS) estimates. This method has not only the key advantage that it provides a computationally cheap closed-form estimator, which guarantees positive definiteness in any case, but also allows applying the proposed order tuning as well as the box constraint tuning discussed in Section V. On the other hand, it should be noted that this method cannot be theoretically guaranteed to yield a local optimum of either the exact or the conditional likelihood.

VII. DUALITY TO BANDING ESTIMATORS

The introduced hyperparameter tuning method in Section V-B fits an AR process with the most suitable order to the given dataset. In this Section, we discuss this method's regularization effect by considering the resulting imposed ICM structure and identify a certain duality to banding estimators, introduced in Section III-B.

The i, j th entry in the ICM of a random vector \mathbf{z} is zero if and only if its i th and j th entry are uncorrelated given all other entries [46]. Thus, by considering a P -dimensional sample from an AR(w) process, with $w < P$, the corresponding ICM is banded by a bandwidth of w . In consequence, by

only allowing $\{\alpha_h\}_{h=0}^{i_{\text{BIC}}-1}$ to be nonzero and due to their relationship to the AR parameters in (40), our proposed order tuning method in Section V-B effectively bands the estimated ICM by a bandwidth of $i_{\text{BIC}}-1$. In contrast, when considering banding estimators, banding is applied to an estimator of the CM, i.e., \mathbf{S}_{avg} in (15). The i, j th entry in the CM of a random vector \mathbf{z} is zero if and only if its i th and j th entry are uncorrelated. When considering a moving-average (MA) process, defined by $X_t = e_t + \sum_{i=1}^w b_i e_{t-i}$ with e_τ being AWGN and parameters $\{b_i\}_{i=1}^w$, the corresponding CM of a P -dimensional sample exhibits a band structure of bandwidth w . Therefore, it is possible to interpret the process of banding \mathbf{S}_{avg} by a bandwidth w as the fitting of a MA(w) process of order w to the given dataset.

As a result, while banding estimators fit a MA process to the given dataset and impose a banding structure on the estimated CM, our proposed estimators fit an AR process and impose a banding structure on the estimated ICM. Due to this duality, we can interpret the regularization effect of both estimators in the same but dual manner. Banding estimators reduce the MSE in situations where the true CM possesses a band structure, i.e., in case of a MA process. However, even in cases where the CM is not inherently banded, this operation introduces a regularization effect by introducing a bias and leveraging the bias-variance trade-off. The same argumentation holds for our proposed estimators in terms of the ICM.

VIII. COMPUTATIONAL COMPLEXITY

The complexity plays a key role for many applications which require the estimation of CMs. This can be due to a high dimensionality but also due to the necessity for low-latency real-time computations [47]. In the following, we will analyze the complexity of optimizing the exact log-likelihood with the box constraints introduced in Section IV-C. We solve it with a projected gradient descent, which consists of two steps constituting the computational complexity, i.e., determining the search direction and the step size.

A. Determining the Search Direction

We start with computing the gradient of the objective $\mathcal{L}_{\mathcal{D}}(\boldsymbol{\alpha})$ defined in (7). The derivative with respect to α_0 is given by

$$\frac{\partial}{\partial \alpha_0} \mathcal{L}_{\mathcal{D}}(\boldsymbol{\alpha}) = \frac{1}{\alpha_0} \text{tr}((\boldsymbol{\Gamma}^{-1} - \mathbf{S})(\mathbf{B} + \mathbf{B}^H - \boldsymbol{\Gamma})). \quad (47)$$

The remaining derivatives are in the real-valued case

$$\frac{\partial}{\partial \alpha_i} \mathcal{L}_{\mathcal{D}}(\boldsymbol{\alpha}) = \frac{2}{\alpha_0} \text{tr}((\boldsymbol{\Gamma}^{-1} - \mathbf{S})(\mathbf{B}(\mathbf{E}^i)^T - \mathbf{Z}(\mathbf{E}^{P-i})^T)) \quad (48)$$

and in the complex-valued case

$$\frac{\partial}{\partial \alpha_i} \mathcal{L}_{\mathcal{D}}(\boldsymbol{\alpha}) = \frac{1}{\alpha_0} \text{tr}((\boldsymbol{\Gamma}^{-1} - \mathbf{S})^T \overline{\mathbf{B}}(\mathbf{E}^i)^T) - \text{tr}((\boldsymbol{\Gamma}^{-1} - \mathbf{S})\mathbf{Z}(\mathbf{E}^{P-i})^T) \quad (49)$$

with $i \in \{1 \dots, P-1\}$, \mathbf{S} being the SCM, \mathbf{B} and \mathbf{Z} given by (5) and (6), and \mathbf{E} being the shift-down matrix. Based on the connection between the GS and the AR parameters in (40),

we can compute $\mathbf{F}(\boldsymbol{\alpha})^{-1}$ by the reversed Levinson algorithm, taking $\mathcal{O}(P^2)$ FLOPs [30, Sec. 6.3.4]. To determine the gradient's complexity, we establish the following Lemmata.

Lemma 5. *Let \mathbf{C}_T be a Hermitian Toeplitz matrix and let \mathbf{D} be a lower triangular Toeplitz matrix and $k \in \{0, \dots, P-1\}$. If $\mathbf{c} = [c_0, \dots, c_{P-1}]^T$ and $\mathbf{d} = [d_0, \dots, d_{P-1}]^T$ denote the first columns of \mathbf{C}_T and \mathbf{D} , respectively, then,*

$$\text{tr}(\mathbf{C}_T \mathbf{D} (\mathbf{E}^k)^T) = \sum_{m=0}^{P-1} \min\{P-k, P-m\} d_m c_{|k-m|}. \quad (50)$$

Proof. See Appendix F. \square

Lemma 6. *Let \mathbf{Q} be any matrix. Moreover, let \mathbf{D} be a lower triangular Toeplitz matrix, $k \in \{0, \dots, P-1\}$ and $\zeta(m) = \min\{P-k-1, P-m-1\}$. If $\mathbf{d} = [d_0, \dots, d_{P-1}]^T$ denote the first column of \mathbf{D} , then,*

$$\text{tr}(\mathbf{Q} \mathbf{D} (\mathbf{E}^k)^T) = \sum_{m=0}^{P-1} d_m \left(\sum_{j=0}^{\zeta(m)} \mathbf{Q}_{k+j, m+j} \right). \quad (51)$$

Proof. See Appendix G. \square

A direct conclusion from Lemma 5 is that the trace in (50) and, thus, the term $\text{tr}(\mathbf{F}^{-1}(\mathbf{B}(\mathbf{E}^i)^T - \mathbf{Z}(\mathbf{E}^{p-i})^T))$ in the real-valued derivative (48) is computable in $\mathcal{O}(P)$ FLOPs. To apply Lemma 6, it is necessary to compute

$$\sum_{j=0}^{\zeta(m)} \mathbf{S}_{k+j, m+j} \text{ for all } k, m = 0, \dots, P-1 \quad (52)$$

with \mathbf{S} being the SCM, which can be precomputed in $\mathcal{O}(P^2)$ FLOPs. Therefore, computing the remaining part of the real-valued gradient $\text{tr}(\mathbf{S}(\mathbf{B}(\mathbf{E}^i)^T - \mathbf{Z}(\mathbf{E}^{p-i})^T))$ in (48) can be done in $\mathcal{O}(P)$ FLOPs according to Lemma 6. The same argumentation can be applied to the complex-valued case in (49). Consequently, the computational complexity of computing the derivatives for all nonzero α_i ($i > 0$) is $\mathcal{O}(P^2)$. The derivative with respect to α_0 in equation (47) needs to be calculated once and requires $\mathcal{O}(P^2)$ FLOPs. Once the gradient is computed, it is projected onto the convex cone of feasible directions to determine the search direction. This projection operation, which guarantees an improving direction [36], takes $\mathcal{O}(P)$ FLOPs. This results in overall $\mathcal{O}(P^2)$ FLOPs of computational cost for the search direction.

B. Determining the Step Size

To determine the step size in the projected gradient descent, we employ the Armijo rule. Since we have calculated the search direction and the gradient beforehand, the only step that adds to the computational complexity is evaluating the objective function at potential candidates for the next iteration. We rewrite the objective function as follows:

$$\mathcal{L}_{\mathcal{D}}(\boldsymbol{\alpha}) = -\log \det \mathbf{F}(\boldsymbol{\alpha})^{-1} - \text{tr}(\mathbf{F} \mathbf{S}) \quad (53)$$

where $\mathbf{F}(\boldsymbol{\alpha})^{-1}$ has also already been computed. To calculate the determinant, we exploit the property that the Cholesky decomposition of a Toeplitz structured CM can be computed in $\mathcal{O}(P^2)$ FLOPs [48]. Additionally, determining the ICM $\mathbf{F}(\boldsymbol{\alpha})$

defined in (4) also takes $\mathcal{O}(P^2)$ FLOPs. This is because the k th off-diagonal of the product of a $P \times P$ triangular Toeplitz matrix with its Hermitian can be recursively computed, requiring $\mathcal{O}(P-k)$ FLOPs. As a result, the overall computational complexity of this product is given by the Gauss summation $\mathcal{O}(\sum_{k=1}^P k) = \mathcal{O}(P^2)$. Consequently, $\mathcal{O}(P^2)$ FLOPs are necessary to evaluate the objective function.

Considering L_B and T_B as the number of iterations for determining the step size and for the projected gradient descent, respectively, the overall computational complexity, without accounting for hyperparameter tuning, is $\mathcal{O}(P^2 L_B T_B)$ FLOPs and, thus, scales quadratically with the samples' dimension.

IX. SIMULATION RESULTS

In the following, we consider different configurations of general WSS AR, MA, and fractional Brownian motion (FBM) processes as ground truth and evaluate the estimators' performance for different numbers N of samples and different dimensions P . As a performance measure, we evaluate the normalized MSE (NMSE) $\mathbb{E}[(\|\hat{\mathbf{A}} - \mathbf{A}\|_{\text{F}}^2) / \|\mathbf{A}\|_{\text{F}}^2]$ ($\mathbf{A} \in \{\mathbf{C}, \mathbf{F}\}$) of the estimated CM $\hat{\mathbf{C}}$ (NMSE_C) and estimated ICM $\hat{\mathbf{F}}$ (NMSE_F) compared to ground truth by averaging over $N_{\text{runs}} = 500$ Monte Carlo runs. In cases where the considered CM estimator does not preserve positive definiteness, we solely evaluate NMSE_C. All estimators we compare ourselves with output an estimate $\hat{\mathbf{C}}$ of the CM rather than an estimate of the inverse. In these cases, the estimated ICM $\hat{\mathbf{F}}$ is computed by inverting $\hat{\mathbf{C}}$, if possible. On the other side, our proposed methods output a parameterization of the ICM $\hat{\mathbf{F}}$ and, thus, in this situation we derive $\hat{\mathbf{C}}$ subsequently by inverting $\hat{\mathbf{F}}$, i.e., $\hat{\mathbf{C}} = \hat{\mathbf{F}}^{-1}$, which takes $\mathcal{O}(P^2)$ FLOPs. The banding and tapering as well as our proposed estimators require hyperparameter tuning. We utilize 4-fold cross validation for tuning the hyperparameter of the banding and tapering estimators in all cases with $N \geq 4$. For $N = 1$, we apply the hyperparameter tuning from [24] and [25]. As windowing function $g(\cdot)$ (cf. Section III-B), we choose the trapezoid function from [21, Sec. 2] with hyperparameter k_T . For the eigenvalue, Frobenius and box constraint estimators proposed in Section IV, we utilize the BIC to tune the order of the fitted AR process, cf. Section V-B. The corresponding likelihood OPs in (21) and (24) are solved by an interior point method. Independently of the process at hand, we use the same class of exponentially decreasing functions \mathcal{F} for the box constraint tuning, cf. Section V-C, i.e.,

$$\mathcal{F} = \{f_m(\eta_m, i)\}_{m=1}^5, \quad (54)$$

with $f_m(\eta_m, i) = \eta_m e^{-\lambda_m i}$ and $i \in \{1, \dots, P-1\}$. The particular values of λ_m and η_m are given in Table I. The parameters η_m are determined by bisection, cf. Section IV-C. Generally, these parameters are dimension-dependent. However, the exponentially decaying behaviour of the functions contained in \mathcal{F} suppresses the GS parameters α_i for large i , independently of the chosen dimension. Consequently, if the dimension is sufficiently large, the parameters η_m can be approximated to be dimension-independent. With the chosen λ_m values, this simplification is valid for dimensions

TABLE I: Chosen parameters of the functions $f_m(\eta_m, i)$ in \mathcal{F} .

m	1	2	3	4	5
λ_m	0.6	1	1.4	1.8	2.2
η_m	0.822	1.718	3.055	5.047	8.025

larger 16, and, therefore, we apply it in our simulations. We use the likelihood as performance measure to determine the best-fitting function in \mathcal{F} . We did not observe noteworthy differences between using the likelihood and k -fold cross validation. Therefore, and because of the disadvantage of leading to a larger computational overhead due to the necessity of computing the estimator k times, we leave out k -fold cross validation in our simulations. For hyperparameter tuning, we continually increase the estimator's degrees of freedom, terminate the process after 5 configurations without increasing hyperparameter performance measure and take the best performing configuration to reduce its computational overhead. The simulation code is publicly available¹.

A. Autoregressive and Moving Average Processes

In Fig. 1, the estimated NMSE of the estimators is shown for the WSS AR(1) process $X_t = aX_{t-1} + e_t$ (a) and b)) and the MA(1) process $X_t = e_t + be_{t-1}$ (c) and d)). In all cases, e_τ is AWGN with variance $\sigma^2 = 0.64$ and from each process we draw $N = 8$ i.i.d. samples, where each sample consists of $P = 16$ successive and therefore correlated realizations of the process. In case of an AR(1) process, the ICM is tridiagonal and the coefficients of the CM decrease exponentially along its off-diagonals, while in case of the MA(1) process it is vice versa.

In Fig. 1 a) and b), the proposed eigenvalue (Eig), Frobenius (Frob), projected gradient descent (PGD) and projected LS (PLS) estimators regularize their estimation without necessarily introducing bias, cf. Section VII, and lead to the best performance. Note that for $N = 8$ and $P = 16$, the ordinary conditional likelihood estimator without projection frequently leads to indefinite ICMs and, thus, cannot be used for CM estimation. PGD and PLS perform slightly better than Eig and Frob, which is due to the box constraint estimators' stronger regularization. In Fig. 1 a), the banding (Band) and tapering (Tape) estimators introduce useful bias due to the CM's exponentially decreasing coefficients, but lead to worse performance than our proposed methods. Due to Band's and Tape's missing guarantee of positive definiteness, they cannot be used for estimating the ICM and are not represented in Fig. 1 b). Although incorporating the true distribution, the likelihood estimators, i.e., \hat{C}_{Circ} Circ and \hat{C}_{EM} EM cannot adapt to the CM's specific characteristics through hyperparameter tuning, which leads to a worse performance in Fig. 1 a) and b) compared to the estimators involving hyperparameter tuning. The estimator S_{avg} Avg in (15) neither involves hyperparameter tuning nor incorporates the distribution and leads in almost all cases in Fig. 1 a) to an even worse performance. The unbiased shrinkage estimator (ShU) is a convex combination of the SCM S and Avg and performs always worse than Avg in Fig. 1 a) due to the imperfect estimation of its convex coefficient. The biased shrinkage estimator (ShB) performs

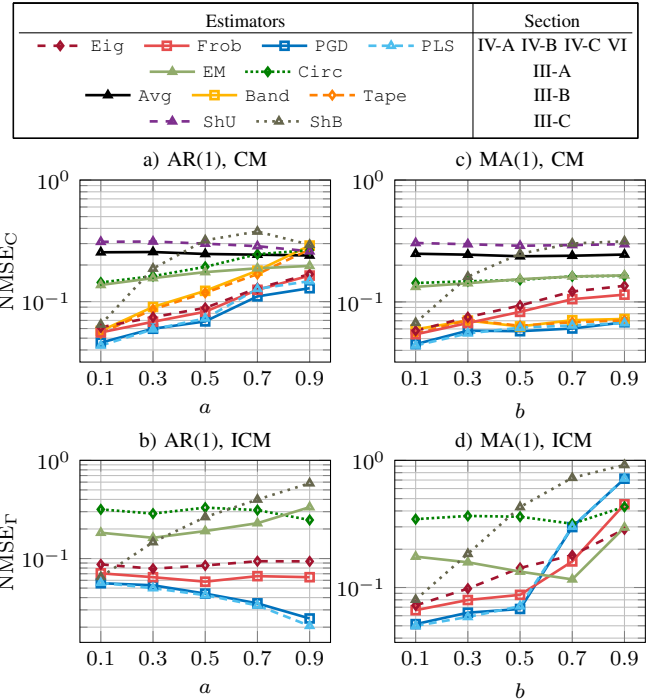


Fig. 1: NMSE of the CM and ICM for an AR(1) process with parameter a , cf. a) and b), and a MA(1) process with parameter b , cf. c) and d). The noise variance is set to 0.64 in all cases, the dimension P is set to 16 and the number N of samples equals 8.

well for $a = 0.1$. This is due to its target matrix T_H in (18), which weights the main-diagonal and all off-diagonals differently and, thus, is able to suppress all off-diagonals in the case of a diagonally dominant CM. However, in all other cases, the equal weighting of all off-diagonal entries introduces a suboptimal bias for the CM's non-negligible off-diagonals and it performs significantly worse. The performance of ShB's estimated ICM can be explained in the same manner.

In case of a MA(1) process in Fig. 1 c) and d), Band and Tape regularize their estimation without necessarily introducing bias, whereas Eig, Frob, PGD and PLS introduce bias, cf. Section VII. However, the latter are likelihood estimators and, thus, have the advantage of incorporating the true distribution in contrast to the former. By exploiting this additional prior knowledge, our estimators diminish their model mismatch of fitting an AR process to the underlying MA process, especially for small b in Fig. 1 c). For larger b , however, the coefficients in the ICM decrease slower in absolute value, leading to a stronger bias of Eig, Frob, PGD and PLS. This results in a worse performance of Eig and Frob, whereas the stronger regularization of PGD and PLS keep their performance in Band's and Tape's performance range. In terms of estimating the ICM in Fig. 1 d) for small b , the estimators' performance can be explained similarly to their performance in Fig. 1 b). For larger b , however, PGD and PLS perform worse than the other likelihood estimators, which can be explained by considering the class of functions \mathcal{F} in (54) used for the box constraint tuning. Generally, λ_m in $f_m(\eta_m, i)$ determines how quickly the bound for $|\alpha_i|$ decays in i . The smaller we choose λ_m in $f_m(\eta_m, i)$, the larger the allowed constraint set is for α_i with large i relative to those with small i . However, the smaller λ_m gets, the smaller η_m has to be to satisfy the constraint in Lemma 3 and, thus, the smaller the constraint

¹<https://github.com/beneboeck/toep-cov-estimation>

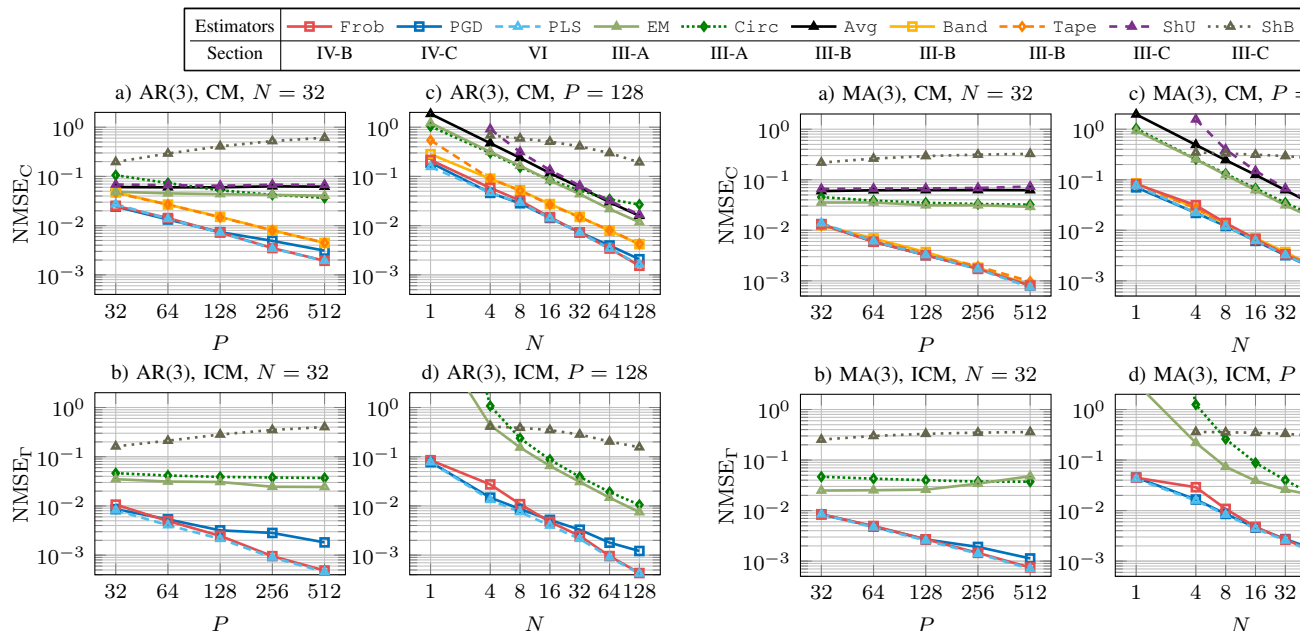


Fig. 2: NMSE for an AR(3) process ($\sigma^2 = 0.64$, $a_1 = 0.5$, $a_2 = 0.2$, $a_3 = 0.05$) with fixed number of samples $N = 32$, cf. a) and b), and with fixed dimension $P = 128$, cf. c) and d).

set generally gets. For a MA(1) process with large b , the true α exhibits a slowly decaying behaviour in its entries and only a small gap exists between α_0 and the remaining α_i ($i = 1, \dots$). In consequence, none of the functions $f_m(\eta_m, i)$ in \mathcal{F} fits rendering \mathcal{F} ill-suited for this specific situation. Additionally, for larger b the stronger bias of Frob, Eig, PGD and PLS worsens their performance in general. From now on, we exclude Eig due to the issues concerning its complexity, cf. Section IV-A.

In Fig. 2, the estimated NMSE of the estimators is given in case of the AR(3) process $X_t = 0.5X_{t-1} + 0.2X_{t-2} + 0.05X_{t-3} + e_t$ for $N = 32$ and varying dimension P , cf. a) and b), as well as $P = 128$ and varying number N of samples, cf. c) and d). In Fig. 3, the same plots are given in case of the MA(3) process $X_t = e_t + 0.5e_{t-1} + 0.2e_{t-2} + 0.05e_{t-3}$. In both cases, e_t is AWGN with variance $\sigma^2 = 0.64$. Generally, the performance of the estimators is consistent with the results for the AR(1) process and the MA(1) process in Fig. 1. For the AR(3) process, our proposed estimators Frob, PGD, and PLS generally perform the best due to their regularization without bias and their consideration of the underlying distribution.

For the CM of the MA(3) process in Fig. 3 a) and c), all estimators incorporating hyperparameter tuning perform approximately the same. Although introducing bias, Frob, PGD, and PLS consider the underlying distribution and, thus, are able to equalize Band's and Tape's better-fitting regularization. For small $N \leq 8$, PGD performs slightly better than Frob, whereas for large $N \geq 32$ it is vice versa. This behaviour is due to the box constraint estimators' smaller constraint set having a strong regularization effect. Although being beneficial for cases with only a few samples N , a strong regularization effect is disadvantageous for larger N , where the estimation's variance is small. Generally, PLS's performance approximately matches the better performance of Frob and PGD. For small N , this is due to having the same strong

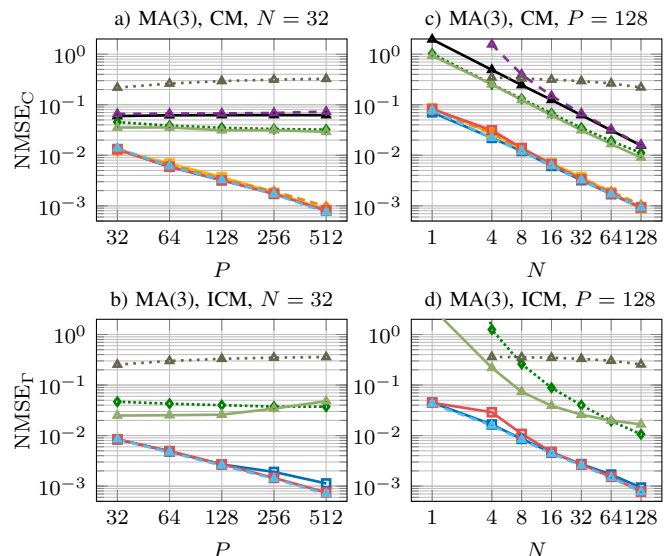


Fig. 3: NMSE for a MA(3) process ($\sigma^2 = 0.64$, $b_1 = 0.5$, $b_2 = 0.2$, $b_3 = 0.05$) with fixed number of samples $N = 32$, cf. a) and b), and with fixed dimension $P = 128$, cf. c) and d).

regularization effect as PGD, whereas for large N or P , finding first the global optimum of the unconstrained conditional likelihood and then projecting onto the box constraints is less restrictive than finding a local optimum within the box constraints.

B. Fractional Brownian Motion

Another WSS process used for modeling long-term dependencies in, e.g., internet traffic, is FBM(h) [49]. The entries in its corresponding CM are defined as

$$C_{ij} = \frac{1}{2} \left((|i-j|+1)^{2h} - 2|i-j|^{2h} + (|i-j|-1)^{2h} \right) \quad (55)$$

where the so-called Hurst parameter h satisfies $h \in [0.5, 1]$. In Fig. 4, the estimated NMSE of the estimators is evaluated in case of the FBM(0.7) process for $N = 32$ and a varying dimension P , cf. a) and b), as well as $P = 128$ and a varying number N of samples, cf. c) and d). The key property of FBM is that the entries of the corresponding CM exhibit a certain saturation in their decline rate, leading to a full CM and ICM with non-negligible entries. In consequence, banding the CM or ICM leads to a larger bias compared to the case of AR or MA processes, and the estimators incorporating hyperparameter tuning do not outperform the ones without in terms of estimating the CM in Fig. 4 a). In Fig. 4 b), Frob, PGD and PLS notably outperform the compared methods since the true α in FBM exhibits a strong decrease along its entries in contrast to the CM's off-diagonals. This leads to a better performing bias when banding the ICM compared to banding the CM. In Fig. 4 c), it can be seen that for small N , the regularization effect of banding the CM and ICM is beneficial due to the high estimation's variance. However, for large N , this regularization is disadvantageous due to the smaller estimation's variance.

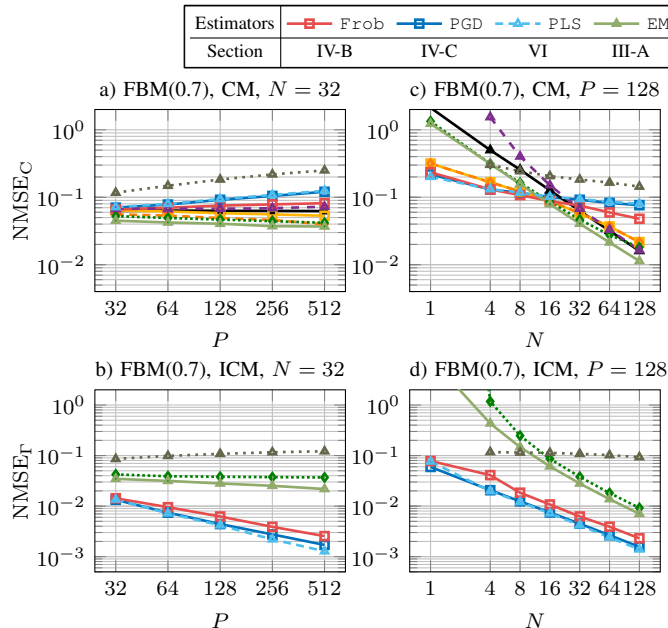


Fig. 4: NMSE for an FBM process ($h = 0.7$) with fixed number of samples $N = 32$, cf. a) and b), and with fixed dimension $P = 128$, cf. c) and d).

C. Complexity and Runtime Analysis

In Fig. 5, the complexity of all estimators (right) and the average measured time in seconds of one estimate for variable dimensions P and fixed number $N = 64$ of samples (left) are given. In both cases, hyperparameter tuning and the computation of the SCM is not considered. The underlying process is an autoregressive moving-average (ARMA)(1,1) process defined as $X_t = 0.7X_{t-1} + e_t + 0.3e_{t-1}$ with $\sigma^2 = 0.64$. For Band and Tape as well as PGD, PLS and Frob, we assume the hyperparameter k_B , k_T and i_{BIC} to be 6, cf. (13) and (41). Additionally, in case of the CM estimators, the measured time as well as the complexity refer to yielding a CM estimate and for our proposed estimators they refer to returning an ICM estimate. The simulations have been conducted on an *Intel Core(TM) i7-1260P (12th Gen)* processor with a base clock speed of 2.1 GHz and all estimators are implemented in *Matlab R2022b*. The computational cost for Band and Tape is linear in P and they are the fastest overall. PLS is also linear in P and can be implemented in $\mathcal{O}(Pi_{BIC} + i_{BIC}^3)$ FLOPs by considering all of its structure. Thus, its complexity is comparable to Band's and Tape's complexity. Estimating the convex coefficient for ShB can be done in $\mathcal{O}(P^2)$ FLOPs, and its measured time is in Band's, Tape's and PLS's range, followed by Avg, also requiring $\mathcal{O}(P^2)$ FLOPs. Although being a likelihood estimator, Circ exhibits a closed-form solution and, thus, does not require an iterative procedure. Moreover, it can be implemented by means of the 2D fast Fourier transform (FFT) in $\mathcal{O}(P^2 \log(P^2))$ FLOPs. Therefore, it is just slightly slower than Avg. PGD is the fastest of all iterative estimators since its complexity scales quadratically in the samples's dimension P , cf. Section VIII. EM exhibits a cubic complexity in the computation of its T_E iterations. In our simulations, however, EM generally required less iterations

Estimators	Frob	PGD	PLS	EM	Circ	Avg	Band	Tape	ShU	ShB
Section	IV-B	IV-C	VI	III-A	III-A	III-B	III-B	III-B	III-C	III-C

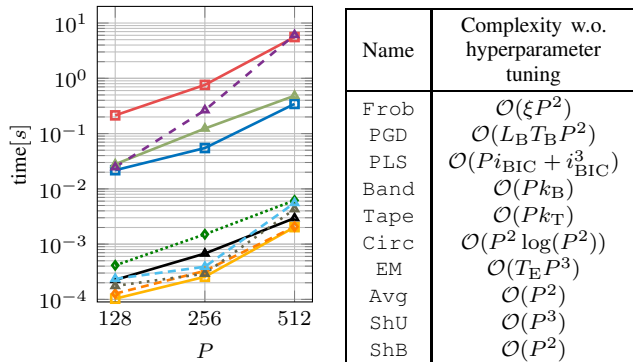


Fig. 5: Left: Measured time without hyperparameter tuning for an ARMA(1,1) process ($\sigma^2 = 0.64$, $a = 0.7$, $b = 0.3$) with a fixed number of samples $N = 64$. Right: Computational complexity without hyperparameter tuning.

than PGD, reducing the gap between these two estimators although having different complexity orders of their individual iterations. In our simulations, we used the interior point method of *Matlab's* built-in optimization function *fmincon* for computing Frob. Moreover, the closed-form solution's complexity of the constraint's gradient can be shown to be cubic in P and, thus, has to be approximated to preserve quadratic complexity. We recognized severe speed ups in terms of measured time, but no decrease in performance due to this approximation. Thus, the update steps of the interior point method can be done in $\mathcal{O}(P^2)$ FLOPs. However, the scaling factor ξ of the interior point method depends on its specific implementation.

X. CONCLUSION

In this work, we presented a novel class of methods yielding likelihood CM and ICM estimators for Toeplitz structured CMs by utilizing the GS decomposition. We derived constraint sets for preserving positive definiteness, leading to well-defined likelihood OPs, and introduced various methods for tuning the hyperparameters and incorporating prior knowledge for this class of estimators. The proposed class of estimators shares the advantage of likelihood estimators, i.e., preserving positive definiteness and considering the underlying distribution, but at the same time includes the advantage of banding and tapering estimators, i.e., an interpretable regularizing method for hyperparameter tuning. Extensive simulations show that the proposed class of estimators significantly outperforms other methods in terms of estimating the ICM. In terms of estimating the CM, they either show comparable or even better performance to the best benchmark estimators, depending on the underlying structure. Moreover, a complexity analysis renders our proposed projected LS estimators to be among the computationally cheapest estimators.

APPENDIX

A. Proof of Lemma 1

We begin with inserting the GS decomposition (4) into the definition of positive definiteness, i.e.,

$$\frac{1}{\alpha_0} (\mathbf{x}^H \mathbf{B} \mathbf{B}^H \mathbf{x} - \mathbf{x}^H \mathbf{Z} \mathbf{Z}^H \mathbf{x}) > 0 \text{ for all } \mathbf{x} \in \mathbb{C}^P, \alpha \in \mathcal{A} \quad (56)$$

with $\mathbf{x} \neq \mathbf{0}$. Note that \mathbf{B} has exactly one eigenvalue $\alpha_0 > 0$ with algebraic multiplicity P . Thus, it has full rank and its range is \mathbb{C}^P . By defining $\mathbf{y} = \mathbf{B}^H \mathbf{x}$, we reformulate (56) as

$$\|\mathbf{y}\|_2^2 - \|\mathbf{Z}^H \mathbf{B}^{-H} \mathbf{y}\|_2^2 > 0 \text{ for all } \mathbf{y} \in \mathbb{C}^P, \alpha \in \mathcal{A} \quad (57)$$

with $\mathbf{y} \neq \mathbf{0}$. By considering the decomposition $\mathbf{y} = \|\mathbf{y}\|_2 \hat{\mathbf{y}}$, multiplying out $\|\mathbf{y}\|_2^2$, and rearranging the terms, we get

$$\|\mathbf{Z}^H \mathbf{B}^{-H} \hat{\mathbf{y}}\|_2^2 < 1 \text{ for all } \hat{\mathbf{y}} \in \mathbb{C}^P \text{ with } \|\hat{\mathbf{y}}\|_2^2 = 1, \alpha \in \mathcal{A} \quad (58)$$

which is equivalent to

$$\max_{\alpha \in \mathcal{A}, \hat{\mathbf{y}} \in \mathbb{C}^P: \|\hat{\mathbf{y}}\|_2^2 = 1} \|\mathbf{Z}^H \mathbf{B}^{-H} \hat{\mathbf{y}}\|_2^2 < 1. \quad (59)$$

The maximization over all $\hat{\mathbf{y}}$ with norm 1 coincides with the definition of the spectral norm, leading to

$$\max_{\alpha \in \mathcal{A}} \|\mathbf{Z}^H \mathbf{B}^{-H}\|_2^2 < 1. \quad (60)$$

B. Proof of Lemma 2

We start by deriving a closed-form solution for \mathbf{B}^{-H} . The work in [34] shows that the inverse of a $P \times P$ lower triangular Toeplitz matrix \mathbf{R} of the following form

$$\mathbf{R}_{ij} = \begin{cases} 0 & \text{if } j > i \\ 1 & \text{if } i = j \\ -r_{|i-j|} & \text{else} \end{cases} \quad (61)$$

with parameters $\mathbf{r} = [r_1, \dots, r_{P-1}]$, is given by

$$(\mathbf{R}^{-1})_{ij} = \begin{cases} 0 & \text{if } j > i \\ 1 & \text{if } i = j \\ F_{i-j}(\mathbf{r}) & \text{else} \end{cases} \quad (62)$$

and $F_i(\mathbf{r})$ is the special case of the generalized Fibonacci sequence defined in (1). By multiplying out α_0 in \mathbf{B} , setting $r_i = -\frac{\alpha_i}{\alpha_0}$ and swapping the indices due to \mathbf{B}^{-H} being upper triangular, we can apply the closed-form solution in (62) to compute

$$(\mathbf{B}^{-H})_{ij} = \begin{cases} 0 & \text{if } i > j \\ \frac{1}{\alpha_0} & \text{if } i = j \\ \frac{1}{\alpha_0} F_{j-i}(-\frac{\alpha_{\geq 1}}{\alpha_0}) & \text{else} \end{cases} \quad (63)$$

with $\alpha_{\geq 1} = [\alpha_1, \dots, \alpha_P]^T$. The matrix \mathbf{Z}^H defined by (6) can be given elementwise by

$$(\mathbf{Z}^H)_{ij} = \begin{cases} \alpha_{P-(j-i)} & \text{if } j > i \\ 0 & \text{else} \end{cases}. \quad (64)$$

Additionally, the matrix $\mathbf{Z}^H \mathbf{B}^{-H}$ exploits the same structure as \mathbf{Z}^H since the multiplication of two upper triangular Toeplitz matrices preserves the structure. Therefore, we define

$$(\mathbf{Z}^H \mathbf{B}^{-H})_{ij} = \begin{cases} g_{j-i} & \text{if } j > i \\ 0 & \text{else} \end{cases}, \quad (65)$$

where $\mathbf{g} = [g_1, \dots, g_{P-1}]$ is fully defined by the first row of $\mathbf{Z}^H \mathbf{B}^{-H}$ and can be elementwise computed by

$$g_k = \sum_{j=1}^{P-1} (\mathbf{Z}^H)_{0j} (\mathbf{B}^{-H})_{jk} = \sum_{j=1}^k \frac{\alpha_{P-j}}{\alpha_0} F_{k-j} \left(-\frac{\alpha_{\geq 1}}{\alpha_0} \right) \quad (66)$$

where we used (64) and the triangular Toeplitz structure of \mathbf{B}^{-H} . Based on (65) we conclude that g_d appears $P-d$ times in $\mathbf{Z}^H \mathbf{B}^{-H}$, rendering the Frobenius norm to be

$$\|\mathbf{Z}^H \mathbf{B}^{-H}\|_F^2 = \sum_{d=1}^{P-1} (P-d) |g_d|^2. \quad (67)$$

C. Proof of Theorem 1

We bound g_k in (66) using the triangular inequality, i.e.,

$$|g_k| \leq \sum_{j=1}^k \left| \frac{\alpha_{P-j}}{\alpha_0} F_{k-j} \left(-\frac{\alpha_{\geq 1}}{\alpha_0} \right) \right|. \quad (68)$$

In the following, we utilize the observation that

$$\left| F_i \left(-\frac{\alpha_{\geq 1}}{\alpha_0} \right) \right| \leq \sum_{l=0}^{i-1} \left| \frac{\alpha_{i-l}}{\alpha_0} \right| \left| F_l \left(-\frac{\alpha_{\geq 1}}{\alpha_0} \right) \right| \leq F_i \left(\left| \frac{\alpha_{\geq 1}}{\alpha_0} \right| \right), \quad (69)$$

where the first inequality comes from the triangular inequality and the definition in (1), and the second inequality results from recursively applying the first inequality. Therefore,

$$\left| \frac{\alpha_{P-j}}{\alpha_0} F_{d-j} \left(-\frac{\alpha_{\geq 1}}{\alpha_0} \right) \right| \leq \left| \frac{\alpha_{P-j}}{\alpha_0} \right| F_{d-j} \left(\left| \frac{\alpha_{\geq 1}}{\alpha_0} \right| \right). \quad (70)$$

We assume to have box constraints $|\alpha_i| \leq K_i \alpha_0$ for all i with $\alpha_0 > 0$. Moreover, by observing that $F_i(\cdot)$ is componentwise monotonically increasing over the domain \mathbb{R}_+^{P-1} , we conclude

$$\left| \frac{\alpha_{P-j}}{\alpha_0} F_{d-j} \left(-\frac{\alpha_{\geq 1}}{\alpha_0} \right) \right| \leq K_{P-j} F_{d-j}(\mathbf{K}) \quad (71)$$

and, according to Lemma 2,

$$\|\mathbf{Z}^H \mathbf{B}^{-H}\|_F^2 \leq B(\mathbf{K}) \quad (72)$$

with $B(\mathbf{K})$ being defined in (29). Since all K_i in (29) are non negative, $B(\mathbf{K})$ is componentwise monotonically increasing in \mathbf{K} . Additionally, $B(\mathbf{K})$ is continuous and equals zero for $\mathbf{K} = \mathbf{0}$. Thus,

$$\exists \mathbf{K} \in \mathbb{R}_+^{P-1} : B(\mathbf{K}) < 1. \quad (73)$$

Based on (72) and Lemma 1, $B(\mathbf{K}) < 1$ implies the GS decomposition $\mathbf{\Gamma}(\alpha)$ in (4) to be PD, concluding the proof.

D. Proof of Lemma 3

Since $B(\mathbf{K})$ is monotonically increasing in each entry of \mathbf{K} and $f(\eta, i)$ is monotonically increasing in η (Property b)), the concatenation $B_f(\eta)$ is monotonically increasing in η as well. Additionally, $f(\eta, i)$ is continuous and equals zero for $\eta = 0$ (Property c)). Therefore, $B_f(\eta)$ is continuous, $B_f(0) = 0$, and

$$\exists \eta \in \mathbb{R}_{++} : B_f(\eta) < 1, \quad (74)$$

which implies $\Gamma(\boldsymbol{\alpha})$ in (4) to be PD and concludes the proof.

E. Proof of Lemma 4

It can be seen that the maximization of $\mathcal{L}_{L|C}(\mathbf{a}, \sigma^2)$ defined in (43) with respect to \mathbf{a} is σ^2 -independent and, thus, equivalent to maximizing

$$-\frac{1}{N} \sum_{n=1}^N \sum_{t=w}^{P-1} |x_t^{(n)} - \sum_{m=1}^w a_m x_{t-m}^{(n)}|^2. \quad (75)$$

Utilizing Wirtinger calculus and setting the derivative of (75) with respect to \bar{a}_j ($j = 1, \dots, w$) to zero yields

$$\frac{1}{N} \sum_{n=1}^N \sum_{t=w}^{P-1} \left(x_t^{(n)} - \sum_{m=1}^w \hat{a}_m x_{t-m}^{(n)} \right) \bar{x}_{t-j}^{(n)} = 0 \quad (76)$$

for all $j = 1, \dots, w$. Rearranging the terms in (76) leads to

$$\sum_{m=1}^w \hat{a}_m \sum_{t=w}^{P-1} \frac{1}{N} \sum_{n=1}^N x_{t-m}^{(n)} \bar{x}_{t-j}^{(n)} = \sum_{t=w}^{P-1} \frac{1}{N} \sum_{n=1}^N x_t^{(n)} \bar{x}_{t-j}^{(n)} \quad (77)$$

for all $j = 1, \dots, w$. By inserting the definition of $\tilde{\mathbf{S}}$ in (45) and rewriting (77) in matrix-vector notation, we end up with

$$\tilde{\mathbf{S}}_{\geq 1, \geq 1} \hat{\mathbf{a}} = \tilde{\mathbf{S}}_{\geq 1, 0}. \quad (78)$$

For deriving the closed form of $\hat{\sigma}^2$ in (44), we first observe that by multiplying (76) with \hat{a}_j and summing over all $j = 1, \dots, w$, we yield

$$\frac{1}{N} \sum_{n=1}^N \sum_{t=w}^{P-1} \left(\left| \sum_{j=1}^w \hat{a}_j x_{t-j}^{(n)} \right|^2 - x_t^{(n)} \sum_{j=1}^w \bar{a}_j \bar{x}_{t-j}^{(n)} \right) = 0. \quad (79)$$

Setting the derivative of $\mathcal{L}_{L|C}(\hat{\mathbf{a}}, \sigma^2)$ with respect to σ^2 to zero and rearranging the terms leads to

$$\hat{\sigma}^2 = \frac{1}{N(P-w)} \sum_{n=1}^N \sum_{t=w}^{P-1} \left| x_t^{(n)} - \sum_{m=1}^w \hat{a}_m x_{t-m}^{(n)} \right|^2 \quad (80)$$

$$= \frac{1}{N(P-w)} \sum_{n=1}^N \sum_{t=w}^{P-1} |x_t^{(n)}|^2 - \bar{x}_t^{(n)} \sum_{m=1}^w \hat{a}_m x_{t-m}^{(n)} - x_t^{(n)} \sum_{m=1}^w \bar{a}_m \bar{x}_{t-m}^{(n)} + \left| \sum_{m=1}^w \hat{a}_m x_{t-m}^{(n)} \right|^2 \quad (81)$$

$$= \frac{1}{N(P-w)} \sum_{n=1}^N \sum_{t=w}^{P-1} |x_t^{(n)}|^2 - \bar{x}_t^{(n)} \sum_{m=1}^w \hat{a}_m x_{t-m}^{(n)}, \quad (82)$$

where the third equality follows from (79). By inserting the definition of $\tilde{\mathbf{S}}$ from (45), we end up with

$$\hat{\sigma}^2 = \frac{1}{P-w} \left(\tilde{\mathbf{S}}_{0,0} - \tilde{\mathbf{S}}_{\geq 1,0}^H \hat{\mathbf{a}} \right) \quad (83)$$

which concludes the proof.

F. Proof of Lemma 5

Let $\tilde{\mathbf{D}} = \mathbf{D}(\mathbf{E}^k)^T$. It can be seen that

$$\tilde{D}_{ij} = \begin{cases} 0 & \text{if } (j < k) \vee (i < j - k) \\ d_{|i-j+k|} & \text{else} \end{cases}. \quad (84)$$

Therefore, we can write

$$\text{tr}(\mathbf{C}_T \mathbf{D}(\mathbf{E}^k)^T) = \sum_{i,j=0}^{P-1} c_{|i-j|} \tilde{D}_{ji} = \sum_{j=k}^{P-1} \sum_{i=j-k}^{P-1} c_{|i-j|} d_{|i-j+k|}. \quad (85)$$

By re-indexing $m = i - j + k$, we get

$$\text{tr}(\mathbf{C}_T \mathbf{D}(\mathbf{E}^k)^T) = \sum_{j=k}^{P-1} \sum_{m=0}^{P-1+k-j} c_{|m-k|} d_m. \quad (86)$$

The double-sum's summation region in the space spanned by the indices j and m corresponds geometrically to a rectangular and a triangular. From this consideration, it can be seen that $\text{tr}(\mathbf{C}_T \mathbf{D}(\mathbf{E}^k)^T)$ equals

$$\begin{aligned} & \sum_{m=0}^{k-1} \sum_{j=k}^{P-1} c_{|m-k|} d_m + \sum_{m=k}^{P-1} \sum_{j=k}^{P-1+k-m} c_{|m-k|} d_m \\ &= (P-k) \sum_{m=0}^{k-1} c_{|m-k|} d_m + \sum_{m=k}^{P-1} (P-m) c_{|m-k|} d_m. \end{aligned} \quad (87)$$

G. Proof of Lemma 6

Similarly to the proof in Appendix F, we start defining $\tilde{\mathbf{D}} = \mathbf{D}(\mathbf{E}^k)^T$, which is given in (84). By following Appendix F and re-indexing $m = k + j$ and $b = j - k$, we get

$$\text{tr}(\mathbf{Q} \mathbf{D}(\mathbf{E}^k)^T) = \sum_{b=0}^{P-1-k} \sum_{m=0}^{P-1-b} \mathbf{Q}_{b+k, b+m} d_m. \quad (88)$$

Similarly to the proof in Appendix F, the double-sum's summation region corresponds to a triangular and a rectangular in the space spanned by the indices m and b . From this consideration, it can be seen that $\text{tr}(\mathbf{Q} \mathbf{D}(\mathbf{E}^k)^T)$ equals

$$\sum_{m=0}^{k-1} d_m \sum_{b=0}^{P-1-k} \mathbf{Q}_{b+k, b+m} + \sum_{m=k}^{P-1} d_m \sum_{b=0}^{P-1-m} \mathbf{Q}_{b+k, b+m}, \quad (89)$$

which concludes the proof.

REFERENCES

- [1] I. Jolliffe, *Principal Component Analysis*. Springer Verlag, 1986.
- [2] T. Kailath, A. Sayed, and B. Hassibi., *Linear estimation*. Upper Saddle River, NJ: Prentice Hall, 2000.
- [3] C. A. Bester, T. G. Conley, and C. B. Hansen, "Inference with dependent data using cluster covariance estimators," *J. Econom.*, vol. 165, no. 2, pp. 137–151, 2011.
- [4] M. Pourahmadi, *High-Dimensional Covariance Estimation*, ser. Wiley Series in Probability and Statistics. John Wiley & Sons, 2013.
- [5] H. Markowitz, "Portfolio selection," *J. Finance*, vol. 7, no. 1, pp. 77–91, 1952.
- [6] J. Guerci, "Theory and application of covariance matrix tapers for robust adaptive beamforming," *IEEE Trans. Signal Process.*, vol. 47, no. 4, pp. 977–985, 1999.
- [7] J. Fan and H. Liu, "Statistical analysis of big data on pharmacogenomics," *Advanced Drug Delivery Reviews*, vol. 65, no. 7, pp. 987–1000, 2013.

- [8] J. Fan, F. Han, and H. Liu, "Challenges of Big Data analysis," *National Science Review*, vol. 1, no. 2, pp. 293–314, 02 2014.
- [9] D. L. Snyder, J. A. O'Sullivan, and M. I. Miller, "The use of maximum likelihood estimation for forming images of diffuse radar targets from delay-Doppler data," *IEEE Trans. Inf. Theory*, vol. 35, pp. 536–548, May 1989.
- [10] D. Fuhrmann, "Application of Toeplitz covariance estimation to adaptive beamforming and detection," *IEEE Trans. Signal Process.*, vol. 39, no. 10, pp. 2194–2198, 1991.
- [11] Y. Ephraim, D. Malah, and B.-H. Juang, "On the application of hidden Markov models for enhancing noisy speech," *IEEE Trans. Acoust., Speech, Signal Process.*, vol. 37, no. 12, pp. 1846–1856, 1989.
- [12] R. Furrer and T. Bengtsson, "Estimation of high-dimensional prior and posterior covariance matrices in Kalman filter variants," *Journal of Multivariate Analysis*, vol. 98, no. 2, pp. 227–255, 2007.
- [13] G. Derado, F. Bowman, and D. K. Clinton, "Modeling the spatial and temporal dependence in fMRI data," *Biometrics*, vol. 66, pp. 949–957, 2010.
- [14] G. L. Stüber, *Principles of Mobile Communication*. Springer International Publishing, 2017.
- [15] K. K. Paliwal, J. G. Lyons, and K. K. Wójcicki, "Preference for 20–40 ms window duration in speech analysis," in *2010 4th Int. Conf. on Signal Process. and Commun. Systems*, 2010, pp. 1–4.
- [16] A. J. Heckens, S. M. Krause, and T. Guhr, "Uncovering the dynamics of correlation structures relative to the collective market motion," *Journal of Statistical Mechanics: Theory and Experiment*, vol. 2020, no. 10, p. 103402, oct 2020.
- [17] T. W. Anderson, "Asymptotically efficient estimation of covariance matrices with linear structure," *The Annals of Statistics*, vol. 1, no. 1, pp. 135 – 141, 1973.
- [18] J. Burg, D. Luenberger, and D. Wenger, "Estimation of structured covariance matrices," *Proceedings of the IEEE*, vol. 70, no. 9, pp. 963–974, 1982.
- [19] M. Miller and D. Snyder, "The role of likelihood and entropy in incomplete-data problems: Applications to estimating point-process intensities and Toeplitz constrained covariances," *Proceedings of the IEEE*, vol. 75, no. 7, pp. 892–907, 1987.
- [20] A. P. Dempster, N. M. Laird, and D. B. Rubin, "Maximum likelihood from incomplete data via the EM algorithm," *Journal of the Royal Statistical Society: Series B (Methodological)*, vol. 39, no. 1, pp. 1–22, 1977.
- [21] T. Cai, Z. Ren, and H. Zhou, "Optimal rates of convergence for estimating Toeplitz covariance matrices," *Probability Theory and Related Fields*, vol. 156, 06 2013.
- [22] P. J. Bickel and E. Levina, "Regularized estimation of large covariance matrices," *The Annals of Statistics*, vol. 36, no. 1, pp. 199 – 227, 2008.
- [23] T. Cai, C. Zhang, and H. Zhou, "Optimal rates of convergence for covariance matrix estimation," *The Annals of Statistics*, vol. 38, no. 4, pp. 2118–2144, 2010.
- [24] W. B. Wu and M. Pourahmadi, "Banding sample autocovariance matrices of stationary processes," *Statistica Sinica*, vol. 19, no. 4, pp. 1755–1768, 2009.
- [25] T. L. McMurry and D. N. Politis, "Banded and tapered estimates for autocovariance matrices and the linear process bootstrap," *Journal of Time Series Analysis*, vol. 31, no. 6, pp. 471–482, 2010.
- [26] P. J. Brockwell and R. A. Davis, *Introduction to Time Series and Forecasting*, ser. Springer Texts in Statistics. Springer International Publishing, 2016.
- [27] T. Lancewicki and M. Aladjem, "Multi-target shrinkage estimation for covariance matrices," *IEEE Trans. Signal Process.*, vol. 62, no. 24, pp. 6380–6390, 2014.
- [28] O. Ledoit and M. Wolf, "A well-conditioned estimator for large-dimensional covariance matrices," *Journal of Multivariate Analysis*, vol. 88, no. 2, pp. 365–411, 2004.
- [29] Y. Chen, A. Wiesel, Y. C. Eldar, and A. O. H. III, "Shrinkage algorithms for MMSE covariance estimation," *IEEE Trans. Signal Process.*, vol. 58, no. 10, pp. 5016–5029, 2010.
- [30] S. Kay, *Modern Spectral Estimation: Theory and Application*, ser. Prentice-Hall signal processing series. Prentice Hall, 1988.
- [31] J. D. Hamilton, *Time Series Analysis*. Princeton University Press, 1994.
- [32] B. N. Mukherjee and S. S. Maiti, "On some properties of positive definite Toeplitz matrices and their possible applications," *Linear Algebra and its Applications*, vol. 102, pp. 211–240, 1988.
- [33] L. McWhorter and L. Scharf, "Nonlinear maximum likelihood estimation of autoregressive time series," *IEEE Trans. Signal Process.*, vol. 43, no. 12, pp. 2909–2919, 1995.
- [34] A. Sahin, "Inverse and factorization of triangular Toeplitz matrices," *Miskolc Mathematical Notes*, vol. 19, p. 527, 01 2018.
- [35] B. Zhang, J. Zhou, and J. Li, "Improved shrinkage estimators of covariance matrices with Toeplitz-structured targets in small sample scenarios," *IEEE Access*, vol. 7, pp. 116 785–116 798, 2019.
- [36] S. Boyd and L. Vandenberghe, *Convex optimization*. Cambridge university press, 2004.
- [37] H. Benson and R. Vanderbei, "Solving problems with semidefinite and related constraints using interior-point methods for nonlinear programming," *Math. Program.*, vol. 95, pp. 279–302, 02 2003.
- [38] T. Kato, *Perturbation Theory for Linear Operators*, 1966.
- [39] A. Lewis, "Derivatives of spectral functions," *Mathematics of Operations Research*, vol. 21, 04 1994.
- [40] F.-R. Lin, W.-K. Ching, and M. K. Ng, "Fast inversion of triangular Toeplitz matrices," *Theoretical Computer Science*, vol. 315, no. 2, pp. 511–523, 2004, algebraic and Numerical Algorithms.
- [41] D. Kucеровsky, K. Mousavand, and A. Sarraf, "On some properties of Toeplitz matrices," *Cogent Mathematics*, vol. 3, no. 1, p. 1154705, 2016.
- [42] G. Kirchgässner and J. Wolters, *Introduction to Modern Time Series Analysis*. Springer Verlag, 01 2007.
- [43] T. Kailath, A. Vieira, and M. Morf, "Inverses of Toeplitz operators, innovations, and orthogonal polynomials," in *1975 IEEE Conf. Decision Control including the 14th Symposium on Adaptive Processes*, 1975, pp. 749–754.
- [44] C. M. Bishop, *Pattern Recognition and Machine Learning (Information Science and Statistics)*, 1st ed. Springer, 2007.
- [45] B. David and G. Bastin, "An estimator of the inverse covariance matrix and its application to ML parameter estimation in dynamical systems," *Automatica*, vol. 37, no. 1, pp. 99–106, 2001.
- [46] J. Friedman, T. Hastie, and R. Tibshirani, "Sparse inverse covariance estimation with the Lasso," *Biostatistics*, vol. 9, 2018.
- [47] D. Neumann, M. Joham, and W. Utschick, "Covariance matrix estimation in massive MIMO," *IEEE Signal Process. Lett.*, vol. 25, no. 6, pp. 863–867, 2018.
- [48] A. W. Bojanczyk, R. P. Brent, F. R. De Hoog, and D. R. Sweet, "On the stability of the Bareiss and related Toeplitz factorization algorithms," *SIAM Journal on Matrix Analysis and Applications*, vol. 16, no. 1, pp. 40–57, 1995.
- [49] W. Leland, M. Taqqu, W. Willinger, and D. Wilson, "On the self-similar nature of ethernet traffic (extended version)," *IEEE/ACM Trans. Netw.*, vol. 2, no. 1, pp. 1–15, 1994.